NANO LETTERS

pubs.acs.org/NanoLett

Letter

Auger Recombination and Carrier–Lattice Thermalization in Semiconductor Quantum Dots under Intense Excitation

Luye Yue, Jingjun Li, Yingpeng Qi, Jie Chen,* Xuan Wang,* and Jianming Cao*

Cite This: *Nano Lett.* 2023, 23, 2578–2585

Read Online

ACCESS | Metrics & More | Article Recommendations | Supporting Information

ABSTRACT: A thorough understanding of the photocarrier relaxation dynamics in semiconductor quantum dots (QDs) is essential to optimize their device performance. However, resolving hot carrier kinetics under high excitation conditions with multiple excitons per dot is challenging because it convolutes several ultrafast processes, including Auger recombination, carrier–phonon scattering, and phonon thermalization. Here, we report a systematic study of the lattice dynamics induced by intense photoexcitation in PbSe QDs. By probing the dynamics from the lattice perspective using ultrafast electron diffraction together with modeling the correlated processes collectively, we can differentiate their roles in photocarrier relaxation. The results reveal that the observed lattice heating time scale is longer than that of carrier intraband relaxation obtained previously using transient optical spectroscopy. Moreover, we find that Auger recombination efficiently annihilates excitons and speeds up lattice heating. This work can be readily extended to other semiconductor QDs systems with varying dot sizes.

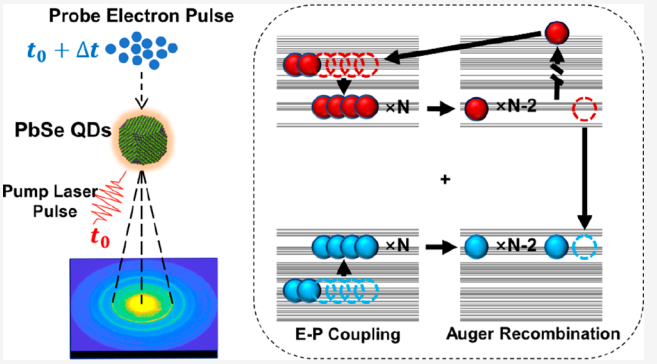

KEYWORDS: *lead selenide quantum dot, multiexciton excitation, electron–phonon coupling, Auger recombination, carrier dynamics, ultrafast electron diffraction*

Due to the unique and size tunable photophysical properties, semiconductor quantum dots are widely used in spectroscopy, solar cells, catalysis, and many other applications.[1−9] The relaxation dynamics of excited carriers affects their device performance, including the switching speed and the luminescence efficiency. A better understanding of carrier cooling, therefore, has significant technological implications. In QDs, space confinement of carriers to several nanometers, comparable to or less than the corresponding exciton Bohr radius, leads to forced overlap of the wave function of carriers, enhances the carrier–carrier interactions, and turns the quasi-continuous energy bands in bulk into discrete levels. As a result, the carrier cooling in QDs differs significantly from that of the corresponding bulk, showing much stronger Auger recombination[10,11] and multiexciton generation effects.[12,13]

Auger recombination is a three-particle process whose rate in QDs is usually characterized by T_N, the lifetime of N exciton state. T_N is proportional to N^{-3}; thus, it can be very short when N is large. Taking a 6 nm PbSe QD as an example, T_N is less than 3 ps when N exceeds 7,[10,14] on a time scale comparable to that of the hot carriers excited by 1.55 eV photons relaxing to the band edge via electron–phonon (E–P) coupling.[15] Thus, it can profoundly interfere with the carrier relaxation, and its effect has been investigated extensively.[16−18] Previously, subpicosecond hot-carrier relaxation in CdSe QDs was observed and attributed to electron–hole Auger-like energy transfer which was thought to be responsible for defeating the effect of a phonon bottleneck.[19,20] Later on, it was reported that Auger recombination reduces the QD LED efficiency significantly and that its effect can be modulated by an intermediate alloyed layer or an additional shell.[21,22] Lately, it was also confirmed that Auger heating dominates the transient lattice heating of semiconductor QDs under a near-bandgap excitation in the absence of localized surface trapping.[23] However, under high excitation conditions, the combined effect as well as the independent contribution from Auger relaxation and E–P coupling to the lattice heating remains unclear. This can largely be attributed to the complexity associated with the convolution of several effects together on an ultrafast time scale, which is manifested as Auger relaxation and E–P coupling occur concurrently and cycle through the entire carrier relaxation process, as shown in Figure 1. Nonetheless, such a multiple-exciton relaxation induced by

Received: December 7, 2022
Revised: March 21, 2023
Published: March 27, 2023

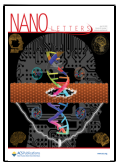

https://doi.org/10.1021/acs.nanolett.2c04804
Nano Lett. 2023, 23, 2578–2585

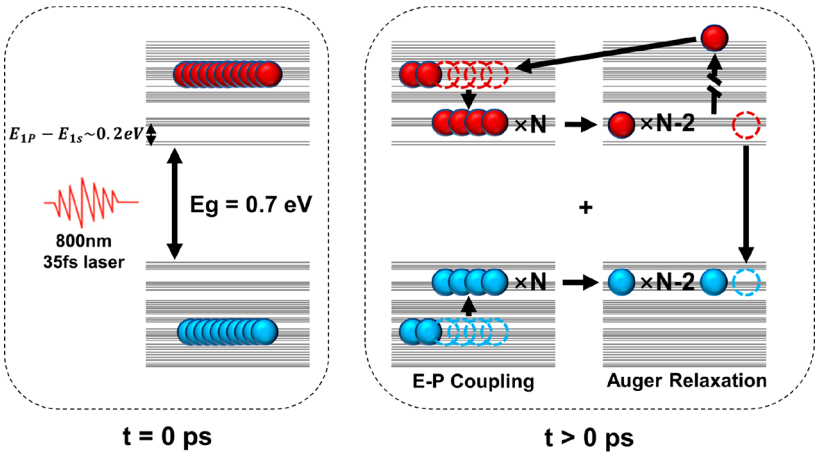

Figure 1. Diagram of hot carriers cooling in 6 nm PbSe QDs under high pump fluence. The left panel shows an initial distribution of electrons and holes at t = 0 ps with $\langle N\rangle_0$ excitons per dot after excitation ($\langle N\rangle_0 \gg 1$). For simplicity, all excitons are assumed to be at the same level. The right panel shows Auger recombination and E−P coupling co-occur within a few picoseconds after the pump. Auger recombination reduces the number of excitons by exciting electrons (holes) to quasi-continuum levels; E−P coupling causes these carriers to relax back to the band edge and release energy to the lattice through emitting phonons.

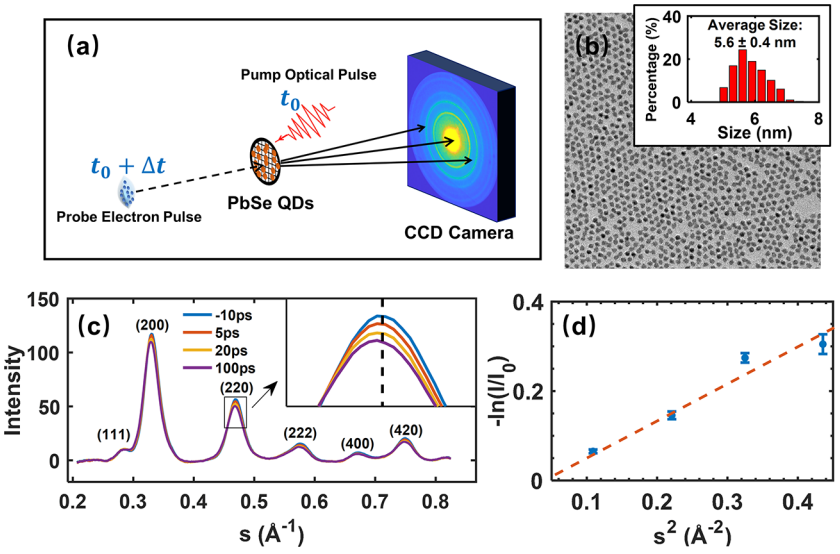

Figure 2. PbSe QDs sample characterization and UED experiment. (a) Diagram of the UED experiment. (b) A TEM image of PbSe QDs. The inset is the dot size distribution. (c) Ultrafast kinetics of Bragg peaks. Inset shows the (220) peak changes at the selected time delays. (d) Logarithm of the quasi-steady intensity $\ln(I/I_0)$ vs the scattering vector squared s^2, where I is the diffraction peak intensity at 100 ps after the time zero and I_0 is the diffraction peak intensity before the time zero. The red dashed line is for guidance.

an intense excitation is essential and directly relevant to many QD applications, including QD lasers,[24,25] high-brightness LEDs,[26,27] and optical amplifiers.[28]

Compared with CdSe QDs, PbSe QDs provide a more desirable system to study hot carrier relaxation under the multiple-exciton condition. The large exciton Bohr radius of 46 nm and large exciton binding energy of tens of millielectronvolts make the quantum confinement effect more significant.[29] Furthermore, the conduction and valence bands of PbSe QDs are nearly identical,[30] effectively minimizing the dominant impact of Auger-like energy transfer via holes on hot carrier relaxation. Previous ultrafast spectroscopy studies on the hot carrier relaxation process of PbSe QDs showed that at the higher quasi-continuous levels the hot carriers are typically coupled with LO phonons with a time constant of less than 500 fs. For carriers at 1S and 1P levels, surface ligands and phonons jointly affect their cooling with a time constant of 1 ps.[31] However, most time-resolved spectral experiments are performed at a lower pumping energy density, with an average number of excitons per dot less than one and nearly no multiexciton interaction.[32] Besides, monitoring carriers usually can only detect their energy depletion but cannot directly determine the amount of the depleted energy and where the energy flows. On the contrary, ultrafast electron diffraction (UED) technique deduces the hot carrier E−P thermalization process from the lattice perspective by directly tracing the magnitude of its transient temperature change. Here we report a systematic study of Auger recombination of multiple excitons in PbSe QDs. The results show that the lattice dynamics of QDs are jointly affected by Auger recombination and E−P coupling. Auger recombination modifies the amount of energy transferred to the lattice and speeds up the lattice heating rates within the first few picoseconds.

https://doi.org/10.1021/acs.nanolett.2c04804
Nano Lett. 2023, 23, 2578−2585

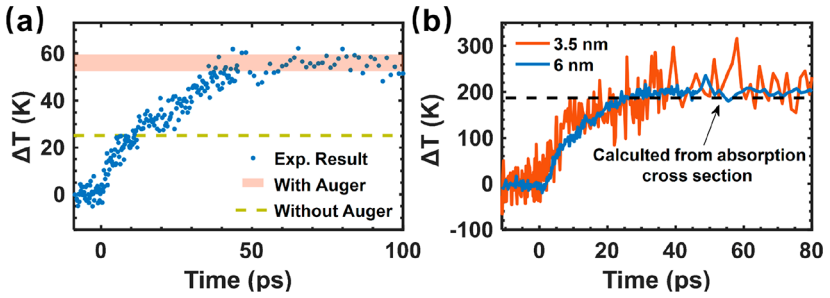

Figure 3. Auger recombination enhances energy flow from excitons to lattice. (a) Transient lattice temperature change at a pump fluence of 1.1 mJ/cm^2 with $\langle N\rangle_0$ = 16. The red-shaded section represents the estimated temperature rise when the Auger recombination exists (number of remaining excitons $\langle N\rangle_{end}$ is no more than 2), and all released energy is transferred to the lattice. The dashed line corresponds to the situation of all excitons accumulated at the band edge without any Auger recombination ($\langle N\rangle_{end}$ = 16). (b) A comparison of ultrafast lattice heating between 3.5 and 6 nm PbSe QDs at a pump fluence of 3.8 mJ/cm^2. The black dashed line represents the equivalent lattice temperature rise if all the absorbed energy is transferred to the lattice.

Figure 2a depicts our pump and probe UED setup. The laser output, which has a pulse energy of 1.0 mJ, a duration of 50 fs, and a wavelength of 800 nm, was divided into two parts. 90% of the output served as the pump beam, while the remaining 10% was frequency-tripled and focused onto a 30 nm thick silver photocathode to generate an ultrashort electron pulse via the photoelectric effect. The pump laser pulse is back-focused on the sample to excite an ultrafast dynamic process, and the probe electron pulse, forming a 170° angle with the pump beam, transmits through the sample to form diffraction patterns for different time delays between the pump and probe. The FWHM of the electron beam at the sample was about 300 μm, 3 times less than that of the pump laser beam of around 0.9 mm, ensuring a uniform sample excitation. The average number of electrons per pulse was set lower than 2000 to maintain an overall time resolution better than 700 fs. More details of our UED system can be found in the Supporting Information and ref 33.

The sample is a layer of high-quality PbSe QDs that were drop-casted uniformly on a TEM grid, as shown in Figures 2b and S2. The average dot size is 5.6 ± 0.4 nm, and the size distribution is shown in the inset. The dot surfaces have been passivated by atomically thin $PbCl_2$ adlayers, improving their stability in air and removing most surface trap states.[34,35] Unless otherwise stated, the sample base temperature is set to 90 K in the UED experiments.

Figure 2c shows the radial profiles of the QD diffraction patterns at several different time delays. The laser-induced changes in both peak position and intensity are clearly seen (see the figure inset). Importantly, $\ln\left(\frac{I}{I_0}\right)$ vs the square of scattering vector s^2 displays a linear dependency (Figure 2d), which indicates that these changes in diffraction patterns arise mainly from the thermal effect of ultrafast lattice heating (see also Figure S5), namely the Debye−Waller (D−W) effect, apart from other possible photoinduced nonthermal effects.[36,37] This observation is consistent with that the lattice temperature deduced from the peak intensity change agrees very well with the value extracted from the peak position shift (Figures S6 and S7). In previous studies, an anomalous feature of the (400) Bragg peak in core/shell[23] and PbS[38] QDs within tens of picoseconds was observed and attributed to the hot carriers captured by the surface trap states. But no such feature was detected in our study because our pump photon energy is lower than the energy threshold (800 nm vs 400 nm) for such dynamical trapping.[23] Also, surface passivation by chlorine quenches the dynamic surface trapping.[38]

Auger recombination serves as a secondary pump, creating carriers with higher excessive energies. Then these carriers can relax to the band edge while transferring energy to the lattice via E−P coupling. Therefore, the overall thermal energy of the lattice should increase compared with the case when Auger recombination is absent. To demonstrate this, we first calculate the overall absorption of QD using the calculated absorption cross section and the measured laser pump fluence. Approximately $\langle N\rangle_0$ = 16 electron−hole pairs are initially excited in a 6 nm QD with a photon energy of 1.55 eV (800 nm). If these carriers are relaxed to the band edge by E−P coupling in the absence of Auger relaxation, the lattice temperature should increase by only about 24 K. However, as shown in Figure 3a, the observed lattice temperature change is about 55 K, corresponding to a condition with approximately one or two averaged electron−hole pairs remaining at the band edge per dot. Collectively, Auger recombination and trapping suppression enhance the energy flow from the carriers to the lattice, resulting in close to 100% of the carrier energy being transferred as thermal energy to the lattice.

To further confirm the effect of Auger recombination, we conducted a UED experiment on a smaller QD of 3.5 ± 0.5 nm whose T_2 and the bandgap are about 40 ps and 1.2 eV,[14] respectively. The measurement was conducted at a higher pump fluence of 3.8 mJ/cm^2 to boost the SNR of 3.5 nm QDs sample data. Because the absorption cross section and volumetric heat capacity are both inversely proportional to the volume of dots,[39] the excited carrier density of a 3.5 nm QD should remain the same as that of 6 nm dots with the same pump fluence (discussed in the Supporting Information Section 2). If all the excited carriers are assumed to relax to and remain at the band edge in the absence of Auger recombination, the lattice temperature change of 3.5 nm QDs should be only about 40% of that of 6 nm QDs because the excessive energy of excited carriers in 3.5 nm QDs is smaller (1.55 eV − 1.2 eV = 0.35 eV for 3.5 nm QDs vs 1.55 eV − 0.7 eV = 0.85 eV for 6 nm QDs). However, as shown in Figure 3b, the lattice temperature changes for both QDs are about the same, around 180 K, which is consistent with the Auger recombination picture. Auger relaxation reduces the number of remained hot carriers and affects their relaxation process. In PbSe QDs, the 1S level, the lowest energy state in the conduction band, is 8-fold degenerate.[40] Therefore, if Auger

https://doi.org/10.1021/acs.nanolett.2c04804
Nano Lett. 2023, 23, 2578−2585

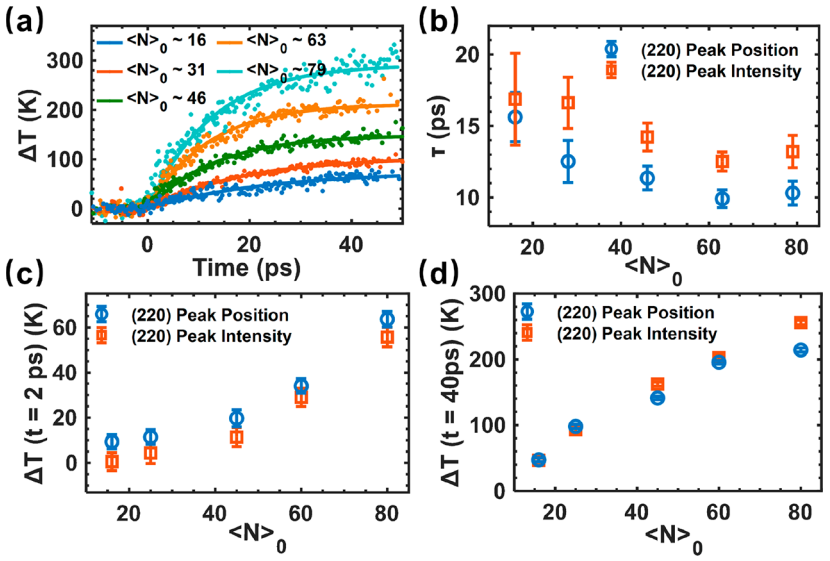

Figure 4. Power-dependent experiments on 6 nm PbSe QDs. (a) Time-dependent lattice temperature kinetics deduced from (220) Bragg peak intensity under different pump fluences. The solid lines are the single exponential fittings. (b) The corresponding lattice heating time constants as a function of $\langle N\rangle_0$. The blue circles are deduced from the (220) peak positions, while the red squares are from the (220) peak intensity. (c) and (d) are extracted lattice temperature variations at 2 and 40 ps after the time zero under different $\langle N\rangle_0$, respectively.

relaxation is not significant, whenever the number of hot carriers exceeds eight, the relaxation of hot carriers to the band edge will be delayed. Our observations, however, show no evidence of such possible two-step lattice heating with a corresponding significantly slower component, which is undesirable for applications such as solar cell or QD laser.

Auger recombination not only increases the amount of energy transferred from excitons to the lattice but also serves as an accelerator for lattice heating. To demonstrate this, the transient lattice temperature variations under different pump fluences are fitted by single-exponential functions to extract the phenomenological time constant of lattice heating (noted as τ), as shown in Figure 4a. Here, the pump fluences are presented as $\langle N\rangle_0$, and the detailed fitting results of other peaks are summarized in Figure S8 and Table S1. Figure 4b depicts τ extracted from either peak position or intensity, both of which decline as the pump fluence increases.

Here, τ is around 13 ps—greater than the value of 2−6 ps measured by transient absorption experiments in the single-exciton case.[15,41,42] The slowdown might not be due to the effect of phonon bottlenecking,[43−45] as it contradicts to the aforementioned reduction of τ at higher pump fluence. We believe that this is largely due to the fact that from the perspective of the lattice, the UED experiment can not only visualize the E−P coupling process but also monitor the intraphonon thermalization, specifically the optical-acoustic phonon thermalization.[46] The intraphonon thermalization is a consequence of mode-dependent E−P interactions, which have been extensively studied.[47−51] Because the phonon thermalization depends on the population of actively involved phonons, the observed τ might be affected through the variation of lattice temperature in our pump-fluence-dependent experiment. To test this, we conducted the UED experiment to extract τ with $\langle N\rangle_0$ = 63 fixed but at a different sample base temperature of 300 K and compared it with that at 90 K (orange curve in Figure 4a). Because the Auger recombination is independent of temperature in the range 90−300 K,[52] only the phonon thermalization might be altered in this case.[53] However, the lattice heating curves under two different sample base temperatures look nearly identical (Figure S9), showing no apparent dependence on sample temperature variation. This is consistent with the works in other semiconducting systems, where the phonon thermalization was found nearly independent of pump fluence.[54,55]

In addition, our results indicate that Auger recombination might enhance the E−P coupling in the first few picoseconds after excitation. Considering that T_N is less than 2 ps when N exceeds 8,[10,14] the majority of excitons will recombine in the first few picoseconds in our experiment. As a result, a large portion of carriers will be excited into higher energy states where quantum confinement is less significant, due to the convergence of electronic structure to a quasi-continuum. Previously, it is found that carriers at higher energy states cool down faster by emitting a single LO phonon with a decay rate of 5 eV/ps than those at lower energy states by emitting multiphonons with a rate of 1 eV/ps.[31] Also, more phonon branches are involved, particularly those lower energy ones, which can speed up lattice heating. On the other hand, the hot phonon bottleneck may be loosened because E−P coupling is no longer restricted to certain optical phonon modes that cause bottleneck. Auger recombination is then expected to cause a more rapid lattice heating only at first several picoseconds, and it should be more pronounced under higher pump fluence. To check this point, we extracted the measured lattice temperature changes ΔT at 2 and 40 ps under different $\langle N\rangle_0$, respectively, which are shown in Figure 4c,d. A nonlinear relationship between the ΔT and pump fluence is clearly seen for ΔT at 2 ps, whereas a linear relationship is established for ΔT at 40 ps. It reflects the cubic relation between Auger recombination rate and the photocarrier density, so that the enhanced exciton annihilation rate is more pronounced at an earlier time for a higher pump. In contrast, on a longer time scale, like 40 ps, the effect of Auger recombination is minor because only 1−2 excitons are remaining at this stage. Above all, in contrast to the low-excitation situation ($\langle N\rangle_0 \sim 2$−3) where Auger recombination could slow down the hot carrier cooling,[56] Auger recombination under a high pump ($\langle N\rangle_0 >$

https://doi.org/10.1021/acs.nanolett.2c04804
Nano Lett. 2023, 23, 2578−2585

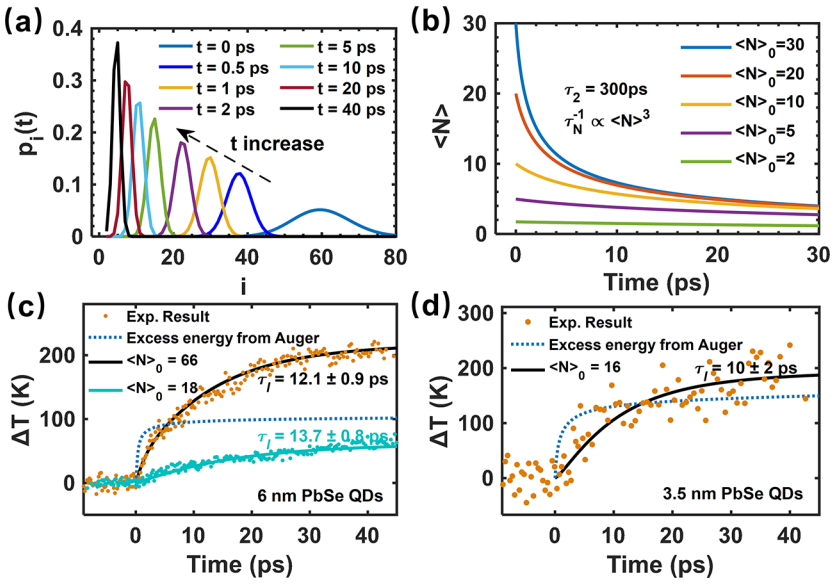

Figure 5. Auger recombination-related lattice heating model. (a) The snapshots of possibility distribution of exciton numbers $p_i(t)$ in a single 6 nm PbSe QD with an initial $\langle N\rangle_0 = 60$ and $T_2 = 100$ ps. Different colors represent different times after the time zero. (b) The average number of excitons in a single QD ($\langle N\rangle$) as a function of delay time. Different colors represent various $\langle N\rangle_0$ with a fixed biexciton lifetime $T_2 = 100$ ps. (c) and (d) compare the experimental results and the transient change of lattice temperature predicted by the lattice heating model. (c) is for 6 nm QDs, and (d) is for 3.5 nm QDs. The dots are experimental data. The blue dotted lines represent the excessive energy of excitons due to Auger recombination. The solid lines are the simulated lattice temperature kinetics with different $\langle N\rangle_0$.

10) could accelerate the carrier energy relaxation and give rise to a faster lattice heating.[57]

To obtain a quantitative analysis of Auger recombination in the observed ultrafast heating of PbSe QDs, we include both Auger recombination and the E−P coupling to model the lattice heating. Figure 1 depicts the physical picture of this coupled process: Auger recombination, which annihilates excitons by creating higher energy carriers, and E−P coupling, which causes excitons to relax back to the band edge by transferring the energy to the lattice. These two processes occur concurrently and cycle through the entire carrier relaxation process under multiexciton excitation conditions, as formulated by the modified two-temperature model below:

$$\frac{dE_{ex}}{dt} = \frac{d\langle N(t)\rangle}{dt} \times E_g - \frac{E_{ex}}{\tau_1} + S(t) \quad (1)$$

$$C_p \frac{dT_l}{dt} = \frac{E_{ex}}{\tau_1} \quad (2)$$

Here, we employ E_{ex} as the excessive energy of the hot exciton and assume that it controls the energy flow to the lattice via carrier−phonon coupling. The first term on the right-hand side of eq 1 depicts the contribution of Auger recombination to lattice heating. The second term represents the exciton−phonon coupling, and one effective time constant τ_1 is utilized to depict the lattice thermalization. Considering the pump laser pulse is very short, the laser pumping ($S(t)$) can be represented by a Dirac delta function: $S(t) = \langle N\rangle_0 * (1.55 - E_g) * \delta(t)$.

Next, the time evolution of $\langle N\rangle$ is simulated using the reported Auger lifetime. The temporal evolution of the probability of i excitons in a QD at time t (noted as $p_i(t)$) is governed by the following rate equations for $i \geq 2$

$$\frac{dp_i(t)}{dt} = \frac{p_{i+1}(t)}{T_{i+1}} - \frac{p_i(t)}{T_i} \quad (3)$$

together with the initial condition $\langle N\rangle_0$ and the biexciton lifetime $T_2 = 100$ ps for 6 nm QDs. We assume $p_i(t = 0)$ obeys the Poisson distribution, as depicted in Figure 5a. It should be noted that for T_2 and T_3 the $T_N^{-1} \propto \langle N\rangle^3$ relation may not hold.[10] However, the violation of cubic relation approximation on small $\langle N\rangle$ has a minor effect when $\langle N\rangle_0$ is quite large (the smallest $\langle N\rangle_0$ is 15.7 in our experiment). The evolution of $p_i(t)$ is shown in Figure 5a, and the time-dependent average exciton number can be calculated by $\langle N(t)\rangle = \sum_{i=0}^{\infty} i p_i(t)$. In Figure 5b, the evolution of $\langle N(t)\rangle$ for different $\langle N\rangle_0$ is obtained by solving the above partial differential equations with the Runge−Kutta method.[58]

We modified the parameters to align the simulated T_l in eq 2 with the experimental data. $\langle N\rangle_0$ was calculated according to the measured temperature jump at 50 ps, and τ_1 is the only fitting parameter. As shown in Figure 5c, T_l agrees well with the experimental data for $\langle N\rangle_0 = 66 \pm 9$, and τ_1 is extracted to be 12.1 ± 0.9 ps. In this figure, the excessive energy of excitons due to Auger relaxation has been converted into an equivalent lattice temperature change (blue dotted line), and the Auger recombination time is substantially shorter than lattice heating, being around 1 ps. From the perspective of the lattice, Auger recombination acts as a secondary pumping source after the excitation laser pulse. The experimental and simulated T_l kinetics under lower $\langle N\rangle_0 = 18.1$ is also plotted to demonstrate how lattice heating accelerates with pump fluence.

We also apply the above lattice heating model to the 3.5 nm QD case, and the results are summarized in Figure 5d. Compared with the 6 nm case, Auger recombination contributes more to the lattice temperature rise, about 80%. The fitted $\langle N\rangle$ is 16 ± 4, and τ_1 is 10 ± 2 ps, a bit smaller than that of 6 nm QDs. It is consistent with the fact that smaller QDs have a larger E−P coupling rate.[59,60] Overall, our model

https://doi.org/10.1021/acs.nanolett.2c04804
Nano Lett. 2023, 23, 2578−2585

produces good overall data fitting and provides a more realistic picture of carrier relaxation dynamics in all-size PbSe QDs under intense excitation.

In conclusion, we applied ultrafast electron diffraction to semiconductor QDs and directly visualized the nonradiative carrier−lattice relaxations in real time with an atomic-scale resolution. By changing experiment conditions such as the dot size and the pump fluence together with theoretical modeling, we unveil the two main aspects of Auger recombination in the lattice heating: it not only increases the amount of energy transferred from the excitons to the lattice but also accelerates lattice heating, especially within the first few picoseconds after excitation. This study provides new insight into the photocarrier relaxation under the strong pump conditions and will help enhance the device performance of relevant semiconductor QDs applications, such as in QDs lasers, high-brightness LEDs, and high-gain optical amplifiers.

■ ASSOCIATED CONTENT

Supporting Information

The Supporting Information is available free of charge at https://pubs.acs.org/doi/10.1021/acs.nanolett.2c04804.

Descriptions of sample preparation and characterization, how to determine the transient temperature change of QDs and the average number of excitons per dot; details of UED experiments under variables including dot size, pump fluence, and sample base temperature (PDF)

■ AUTHOR INFORMATION

Corresponding Authors

Jie Chen − *Center for Ultrafast Science and Technology, Key Laboratory for Laser Plasmas (Ministry of Education) and School of Physics and Astronomy, Shanghai Jiao Tong University, Shanghai 200240, China;* orcid.org/0000-0001-5983-7479; Email: jiec@sjtu.edu.cn

Xuan Wang − *Beijing National Laboratory for Condensed Matter Physics, Institute of Physics, Chinese Academy of Sciences, Beijing 100190, China; Songshan Lake Materials Laboratory, Dongguan, Guangdong 523808, China;* Email: xw@iphy.ac.cn

Jianming Cao − *Physics Department and National High Magnetic Field Laboratory, Florida State University, Tallahassee, Florida 32310, United States; Center for Ultrafast Science and Technology, Key Laboratory for Laser Plasmas (Ministry of Education) and School of Physics and Astronomy, Shanghai Jiao Tong University, Shanghai 200240, China;* Email: jcao@magnet.fsu.edu

Authors

Luye Yue − *Center for Ultrafast Science and Technology, Key Laboratory for Laser Plasmas (Ministry of Education) and School of Physics and Astronomy, Shanghai Jiao Tong University, Shanghai 200240, China;* orcid.org/0000-0002-4483-108X

Jingjun Li − *Center for Ultrafast Science and Technology, Key Laboratory for Laser Plasmas (Ministry of Education) and School of Physics and Astronomy, Shanghai Jiao Tong University, Shanghai 200240, China*

Yingpeng Qi − *Center for Ultrafast Science and Technology, Key Laboratory for Laser Plasmas (Ministry of Education) and School of Physics and Astronomy, Shanghai Jiao Tong University, Shanghai 200240, China;* orcid.org/0000-0001-5950-8157

Complete contact information is available at: https://pubs.acs.org/10.1021/acs.nanolett.2c04804

Author Contributions

L.Y., J.C., X.W., and J.C. conceived the project and designed the experiments; L.Y., J.L., and Y.Q. performed the experiments; L.Y., J.C., X.W., and J.C. wrote the paper. All authors have given approval to the final version of the manuscript.

Notes

The authors declare no competing financial interest.

■ ACKNOWLEDGMENTS

We acknowledge Jianbing Zhang's group in the School of Optical and Electronic Information of Huazhong University of Science and Technology (HUST) in China for QD synthesis. This work is supported by the National Natural Science Foundation of China under Grant 11774409, the National Natural Science Foundation of China under Grant 11974241, the Youth Program of National Natural Science Foundation of China under Grant 11904394, US-NSF Cooperative agreement (Grants DMR-1644779 and DMR-2128556), and the state of Florida. We also thank the UED experimental station under the Synergetic Extreme Condition User Facility (SECUF) in China.

■ REFERENCES

(1) Li, X.; Wu, Y.; Steel, D.; Gammon, D.; Stievater, T. H.; Katzer, D. S.; Park, D.; Piermarocchi, C.; Sham, L. J. An All-Optical Quantum Gate in a Semiconductor Quantum Dot. *Science* **2003**, *301* (5634), 809−811.

(2) Masumoto, Y.; Takagahara, T. *Semiconductor Quantum Dots: Physics, Spectroscopy and Applications*; Springer Science & Business Media: 2013.

(3) Garcia de Arquer, F. P.; Talapin, D. V.; Klimov, V. I.; Arakawa, Y.; Bayer, M.; Sargent, E. H. Semiconductor Quantum Dots: Technological Progress and Future Challenges. *Science* **2021**, *373* (6555), No. eaaz8541.

(4) Nozik, A. J. Spectroscopy and Hot Electron Relaxation Dynamics in Semiconductor Quantum Wells and Quantum Dots. *Annu. Rev. Phys. Chem.* **2001**, *52*, 193−231.

(5) Berthelot, A.; Favero, I.; Cassabois, G.; Voisin, C.; Delalande, C.; Roussignol, Ph.; Ferreira, R.; Gérard, J. M. Unconventional Motional Narrowing in the Optical Spectrum of a Semiconductor Quantum Dot. *Nat. Phys.* **2006**, *2* (11), 759−764.

(6) Semonin, O. E.; Luther, J. M.; Choi, S.; Chen, H.-Y.; Gao, J.; Nozik, A. J.; Beard, M. C. Peak External Photocurrent Quantum Efficiency Exceeding 100% via MEG in a Quantum Dot Solar Cell. *Science* **2011**, *334* (6062), 1530−1533.

(7) Zhang, J.; Gao, J.; Church, C. P.; Miller, E. M.; Luther, J. M.; Klimov, V. I.; Beard, M. C. PbSe Quantum Dot Solar Cells with More than 6% Efficiency Fabricated in Ambient Atmosphere. *Nano Lett.* **2014**, *14* (10), 6010−6015.

(8) Weiss, E. A. Designing the Surfaces of Semiconductor Quantum Dots for Colloidal Photocatalysis. *ACS Energy Lett.* **2017**, *2* (5), 1005−1013.

(9) Caputo, J. A.; Frenette, L. C.; Zhao, N.; Sowers, K. L.; Krauss, T. D.; Weix, D. J. General and Efficient C-C Bond Forming Photoredox Catalysis with Semiconductor Quantum Dots. *J. Am. Chem. Soc.* **2017**, *139* (12), 4250−4253.

(10) Klimov, V. I.; McGuire, J. A.; Schaller, R. D.; Rupasov, V. I. Scaling of Multiexciton Lifetimes in Semiconductor Nanocrystals. *Physical Review B - Condensed Matter and Materials Physics* **2008**, *77* (19), 1−12.

(11) Klimov, V. I.; Mikhailovsky, A. A.; McBranch, D. W.; Leatherdale, C. A.; Bawendi, M. G. Quantization of Multiparticle Auger Rates in Semiconductor Quantum Dots. *Science* **2000**, *287* (5455), 1011−1014.
(12) Schaller, R. D.; Petruska, M. A.; Klimov, V. I. Effect of Electronic Structure on Carrier Multiplication Efficiency: Comparative Study of PbSe and CdSe Nanocrystals. *Appl. Phys. Lett.* **2005**, *87* (25), 1−3.
(13) Mcguire, J. A.; Joo, J.; Pietryga, J. M.; Schaller, R. D.; Klimov, V. I. New Aspects of Carrier Multiplication in Semiconductor Nanocrystals. *Acc. Chem. Res.* **2008**, *41* (12), 1810−1819.
(14) Luther, J. M.; Beard, M. C.; Song, Q.; Law, M.; Ellingson, R. J.; Nozik, A. J. Multiple Exciton Generation in Films of Electronically Coupled PbSe Quantum Dots. *Nano Lett.* **2007**, *7* (6), 1779−1784.
(15) Schaller, R. D.; Pietryga, J. M.; Goupalov, S. V.; Petruska, M. A.; Ivanov, S. A.; Klimov, V. I. Breaking the Phonon Bottleneck in Semiconductor Nanocrystals via Multiphonon Emission Induced by Intrinsic Nonadiabatic Interactions. *Phys. Rev. Lett.* **2005**, *95* (19), 1−4.
(16) Park, Y. S.; Bae, W. K.; Pietryga, J. M.; Klimov, V. I. Auger Recombination of Biexcitons and Negative and Positive Trions in Individual Quantum Dots. *ACS Nano* **2014**, *8* (7), 7288−7296.
(17) Seiler, H.; Palato, S.; Sonnichsen, C.; Baker, H.; Kambhampati, P. Seeing Multiexcitons through Sample Inhomogeneity: Band-Edge Biexciton Structure in CdSe Nanocrystals Revealed by Two-Dimensional Electronic Spectroscopy. *Nano Lett.* **2018**, *18* (5), 2999−3006.
(18) Walsh, B. R.; Sonnichsen, C.; MacK, T. G.; Saari, J. I.; Krause, M. M.; Nick, R.; Coe-Sullivan, S.; Kambhampati, P. Excited State Phononic Processes in Semiconductor Nanocrystals Revealed by Excitonic State-Resolved Pump/Probe Spectroscopy. *J. Phys. Chem. C* **2019**, *123* (6), 3868−3875.
(19) Efros, Al. L.; Kharchenko, V. A.; Rosen, M. Breaking the Phonon Bottleneck in Nanometer Quantum Dots: Role of Auger-like Processes. *Solid State Commun.* **1995**, *93* (4), 281−284.
(20) Guyot-Sionnest, P.; Shim, M.; Matranga, C.; Hines, M. Intraband Relaxation in CdSe Quantum Dots. *Phys. Rev. B* **1999**, *60* (4), R2181−R2184.
(21) Bae, W. K.; Park, Y.-S.; Lim, J.; Lee, D.; Padilha, L. A.; McDaniel, H.; Robel, I.; Lee, C.; Pietryga, J. M.; Klimov, V. I. Controlling the Influence of Auger Recombination on the Performance of Quantum-Dot Light-Emitting Diodes. *Nat. Commun.* **2013**, *4* (1), 2661.
(22) Hou, X.; Kang, J.; Qin, H.; Chen, X.; Ma, J.; Zhou, J.; Chen, L.; Wang, L.; Wang, L.-W.; Peng, X. Engineering Auger Recombination in Colloidal Quantum Dots via Dielectric Screening. *Nat. Commun.* **2019**, *10* (1), 1750.
(23) Guzelturk, B.; Cotts, B. L.; Jasrasaria, D.; Philbin, J. P.; Hanifi, D. A.; Koscher, B. A.; Balan, A. D.; Curling, E.; Zajac, M.; Park, S.; Yazdani, N.; Nyby, C.; Kamysbayev, V.; Fischer, S.; Nett, Z.; Shen, X.; Kozina, M. E.; Lin, M.-F.; Reid, A. H.; Weathersby, S. P.; Schaller, R. D.; Wood, V.; Wang, X.; Dionne, J. A.; Talapin, D. V.; Alivisatos, A. P.; Salleo, A.; Rabani, E.; Lindenberg, A. M. Dynamic Lattice Distortions Driven by Surface Trapping in Semiconductor Nanocrystals. *Nat. Commun.* **2021**, *12* (1), 1860.
(24) Klimov, V. I. Mechanisms for Photogeneration and Recombination of Multiexcitons in Semiconductor Nanocrystals: Implications for Lasing and Solar Energy Conversion. *J. Phys. Chem. B* **2006**, *110* (34), 16827−16845.
(25) Rafailov, E. U.; Cataluna, M. A.; Sibbett, W. Mode-Locked Quantum-Dot Lasers. *Nat. Photonics* **2007**, *1* (7), 395−401.
(26) Caruge, J. M.; Halpert, J. E.; Wood, V.; Bulović, V.; Bawendi, M. G. Colloidal Quantum-Dot Light-Emitting Diodes with Metal-Oxide Charge Transport Layers. *Nat. Photonics* **2008**, *2* (4), 247−250.
(27) Pal, B. N.; Ghosh, Y.; Brovelli, S.; Laocharoensuk, R.; Klimov, V. I.; Hollingsworth, J. A.; Htoon, H. Giant" CdSe/CdS Core/Shell Nanocrystal Quantum Dots as Efficient Electroluminescent Materials: Strong Influence of Shell Thickness on Light-Emitting Diode Performance. *Nano Lett.* **2012**, *12* (1), 331−336.
(28) Schaller, R. D.; Petruska, M. A.; Klimov, V. I. Tunable Near-Infrared Optical Gain and Amplified Spontaneous Emission Using PbSe Nanocrystals. *J. Phys. Chem. B* **2003**, *107* (50), 13765−13768.
(29) Wise, F. W. Lead Salt Quantum Dots: The Limit of Strong Quantum Confinement. *Acc. Chem. Res.* **2000**, *33* (11), 773−780.
(30) An, J. M.; Franceschetti, A.; Dudiy, S. V.; Zunger, A. The Peculiar Electronic Structure of PbSe Quantum Dots. *Nano Lett.* **2006**, *6* (12), 2728−2735.
(31) Spoor, F. C. M.; Tomić, S.; Houtepen, A. J.; Siebbeles, L. D. A. Broadband Cooling Spectra of Hot Electrons and Holes in PbSe Quantum Dots. *ACS Nano* **2017**, *11* (6), 6286−6294.
(32) Klimov, V. I. Optical Nonlinearities and Ultrafast Carrier Dynamics in Semiconductor Nanocrystals. *J. Phys. Chem. B* **2000**, *104* (26), 6112−6123.
(33) Li, R.; Zhu, P.; Chen, J.; Cao, J.; Rentzepis, P. M.; Zhang, J. Direct Observation of Ultrafast Thermal and Non-Thermal Lattice Deformation of Polycrystalline Aluminum Film. *Appl. Phys. Lett.* **2017**, *111* (4), 0−12.
(34) Zhang, J.; Gao, J.; Miller, E. M.; Luther, J. M.; Beard, M. C. Diffusion-Controlled Synthesis of PbS and PbSe Quantum Dots with in Situ Halide Passivation for Quantum Dot Solar Cells. *ACS Nano* **2014**, *8* (1), 614−622.
(35) Lian, L.; Xia, Y.; Zhang, C.; Xu, B.; Yang, L.; Liu, H.; Zhang, D.; Wang, K.; Gao, J.; Zhang, J. In Situ Tuning the Reactivity of Selenium Precursor to Synthesize Wide Range Size, Ultralarge-Scale, and Ultrastable PbSe Quantum Dots. *Chem. Mater.* **2018**, *30* (3), 982−989.
(36) Cao, G.; Sun, S.; Li, Z.; Tian, H.; Yang, H.; Li, J. Clocking the Anisotropic Lattice Dynamics of Multi-Walled Carbon Nanotubes by Four-Dimensional Ultrafast Transmission Electron Microscopy. *Sci. Rep.* **2015**, *5*, 1−7.
(37) Esmail, A. R.; Bugayev, A.; Elsayed-Ali, H. E. Electron Diffraction Studies of Structural Dynamics of Bismuth Nanoparticles. *J. Phys. Chem. C* **2013**, *117* (17), 9035−9041.
(38) Krawczyk, K. M.; Sarracini, A.; Green, P. B.; Hasham, M.; Tang, K.; Paré-Labrosse, O.; Voznyy, O.; Wilson, M. W. B.; Miller, R. J. D. Anisotropic, Nonthermal Lattice Disordering Observed in Photoexcited PbS Quantum Dots. *J. Phys. Chem. C* **2021**, *125* (40), 22120−22132.
(39) Moreels, I.; Lambert, K.; De Muynck, D.; Vanhaecke, F.; Poelman, D.; Martins, J. C.; Allan, G.; Hens, Z. Composition and Size-Dependent Extinction Coefficient of Colloidal PbSe Quantum Dots. *Chem. Mater.* **2007**, *19* (25), 6101−6106.
(40) Allan, G.; Delerue, C. Confinement Effects in PbSe Quantum Wells and Nanocrystals. *Physical Review B - Condensed Matter and Materials Physics* **2004**, *70* (24), 1−9.
(41) Wehrenberg, B. L.; Wang, C.; Guyot-Sionnest, P. Interband and Intraband Optical Studies of PbSe Colloidal Quantum Dots. *J. Phys. Chem. B* **2002**, *106* (41), 10634−10640.
(42) Miaja-Avila, L.; Tritsch, J. R.; Wolcott, A.; Chan, W. L.; Nelson, C. A.; Zhu, X. Y. Direct Mapping of Hot-Electron Relaxation and Multiplication Dynamics in PbSe Quantum Dots. *Nano Lett.* **2012**, *12* (3), 1588−1591.
(43) Heitz, R.; Born, H.; Guffarth, F.; Stier, O.; Schliwa, A.; Hoffmann, A.; Bimberg, D. Existence of a Phonon Bottleneck for Excitons in Quantum Dots. *Physical Review B - Condensed Matter and Materials Physics* **2001**, *64* (24), 1−4.
(44) Yang, J.; Wen, X.; Xia, H.; Sheng, R.; Ma, Q.; Kim, J.; Tapping, P.; Harada, T.; Kee, T. W.; Huang, F.; Cheng, Y.-B.; Green, M.; Ho-Baillie, A.; Huang, S.; Shrestha, S.; Patterson, R.; Conibeer, G. Acoustic-Optical Phonon up-Conversion and Hot-Phonon Bottleneck in Lead-Halide Perovskites. *Nat. Commun.* **2017**, *8* (1), 14120.
(45) Wang, L.; Chen, Z.; Liang, G.; Li, Y.; Lai, R.; Ding, T.; Wu, K. Observation of a Phonon Bottleneck in Copper-Doped Colloidal Quantum Dots. *Nat. Commun.* **2019**, *10* (1), 1−8.
(46) Harvey, S. M.; Phelan, B. T.; Hannah, D. C.; Brown, K. E.; Young, R. M.; Kirschner, M. S.; Wasielewski, M. R.; Schaller, R. D. Auger Heating and Thermal Dissipation in Zero-Dimensional CdSe

https://doi.org/10.1021/acs.nanolett.2c04804
Nano Lett. 2023, 23, 2578−2585

Nanocrystals Examined Using Femtosecond Stimulated Raman Spectroscopy. *J. Phys. Chem. Lett.* **2018**, *9* (16), 4481−4487.
(47) René de Cotret, L. P.; Pöhls, J.-H.; Stern, M. J.; Otto, M. R.; Sutton, M.; Siwick, B. J. Time- and Momentum-Resolved Phonon Population Dynamics with Ultrafast Electron Diffuse Scattering. *Phys. Rev. B* **2019**, *100* (21), 214115.
(48) Zacharias, M.; Seiler, H.; Caruso, F.; Zahn, D.; Giustino, F.; Kelires, P. C.; Ernstorfer, R. Multiphonon Diffuse Scattering in Solids from First Principles: Application to Layered Crystals and Two-Dimensional Materials. *Phys. Rev. B* **2021**, *104* (20), 1−16.
(49) Krishnamoorthy, A.; Lin, M. F.; Zhang, X.; Weninger, C.; Ma, R.; Britz, A.; Tiwary, C. S.; Kochat, V.; Apte, A.; Yang, J.; Park, S.; Li, R.; Shen, X.; Wang, X.; Kalia, R.; Nakano, A.; Shimojo, F.; Fritz, D.; Bergmann, U.; Ajayan, P.; Vashishta, P. Optical Control of Non-Equilibrium Phonon Dynamics. *Nano Lett.* **2019**, *19* (8), 4981−4989.
(50) Sadasivam, S.; Chan, M. K. Y.; Darancet, P. Theory of Thermal Relaxation of Electrons in Semiconductors. *Phys. Rev. Lett.* **2017**, *119* (13), 136602.
(51) Tong, X.; Bernardi, M. Toward Precise Simulations of the Coupled Ultrafast Dynamics of Electrons and Atomic Vibrations in Materials. *Phys. Rev. Research* **2021**, *3* (2), 023072.
(52) Kobayashi, Y.; Tamai, N. Size-Dependent Multiexciton Spectroscopy and Moderate Temperature Dependence of Biexciton Auger Recombination in Colloidal CdTe Quantum Dots. *J. Phys. Chem. C* **2010**, *114* (41), 17550−17556.
(53) Zahn, D.; Hildebrandt, P. N.; Vasileiadis, T.; Windsor, Y. W.; Qi, Y.; Seiler, H.; Ernstorfer, R. Anisotropic Nonequilibrium Lattice Dynamics of Black Phosphorus. *Nano Lett.* **2020**, *20* (5), 3728−3733.
(54) Song, D.; Wang, F.; Dukovic, G.; Zheng, M.; Semke, E. D.; Brus, L. E.; Heinz, T. F. Direct Measurement of the Lifetime of Optical Phonons in Single-Walled Carbon Nanotubes. *Phys. Rev. Lett.* **2008**, *100* (22), 225503.
(55) Wu, S.; Liu, W.-T.; Liang, X.; Schuck, P. J.; Wang, F.; Shen, Y. R.; Salmeron, M. Hot Phonon Dynamics in Graphene. *Nano Lett.* **2012**, *12* (11), 5495−5499.
(56) Achermann, M.; Bartko, A. P.; Hollingsworth, J. A.; Klimov, V. I. The Effect of Auger Heating on Intraband Carrier Relaxation in Semiconductor Quantum Rods. *Nat. Phys.* **2006**, *2* (8), 557−561.
(57) Winzer, T.; Malić, E. Impact of Auger Processes on Carrier Dynamics in Graphene. *Physical Review B - Condensed Matter and Materials Physics* **2012**, *85* (24), 1−5.
(58) Robel, I.; Gresback, R.; Kortshagen, U.; Schaller, R. D.; Klimov, V. I. Universal Size-Dependent Trend in Auger Recombination in Direct-Gap and Indirect-Gap Semiconductor Nanocrystals. *Phys. Rev. Lett.* **2009**, *102* (17), 1−4.
(59) Klimov, V. I.; Mcbranch, D. W. Femtosecond 1P-to-1S Electron Relaxation in Strongly Confined Semiconductor Nanocrystals. *Phys. Rev. Lett.* **1998**, *80*, 4028−4031.
(60) Kambhampati, P. Unraveling the Structure and Dynamics of Excitons in Semiconductor Quantum Dots. *Acc. Chem. Res.* **2011**, *44* (1), 1−13.

https://doi.org/10.1021/acs.nanolett.2c04804
Nano Lett. 2023, 23, 2578−2585